Surface superconductivity, positive field cooled magnetization, and peak-effect phenomenon observed in a spherical single crystal of niobium

Pradip Das,[1] C. V. Tomy,[1,*] S. S. Banerjee,[2,†] H. Takeya,[3] S. Ramakrishnan,[4] and A. K. Grover[4,‡]
[1]*Department of Physics, Indian Institute of Technology Bombay, Mumbai 400076, India*
[2]*Department of Physics, Indian Institute of Technology Kanpur, Kanpur 208016, India*
[3]*National Institute of Materials Science, Ibaraki 305-0047, Japan*
[4]*Department of Condensed Matter Physics and Materials Science, Tata Institute of Fundamental Research, Mumbai 400 005, India*
(Received 19 July 2008; revised manuscript received 12 September 2008; published 3 December 2008)

We report the observation of surface superconductivity as well as positive field cooled magnetization, along with peak-effect phenomenon in ac and dc magnetization measurements in a high-purity spherical single crystal of niobium. We study how the surface superconductivity and the positive field cooled magnetization evolve over the field (H) and the temperature (T) phase space. We suggest that the observed evolution in the strength of the positive field cooled magnetization signal may be understood on the basis of the temperature dependence of the superconducting coherence length.

DOI: 10.1103/PhysRevB.78.214504 PACS number(s): 74.25.Qt, 74.25.Dw, 73.25.+i

I. INTRODUCTION

Elemental niobium (a type-II superconductor with $T_c \sim 9.3$ K) has long been[1–4] one of the favored materials to study the characteristics of vortex matter[5,6] in superconductors. In recent years, single crystals of Nb have been extensively probed[7–11] in the context of vortex phase diagram studies, viz., the symmetry of the flux line lattice (FLL) and the spatial correlations among collectively pinned vortices. Some subtle effects[8,11] related to the vortex matter have surfaced up only in near ideal conditions, such as in ultrapure single crystal of Nb. Examples of these include the recent observation of the symmetry of crystalline lattice competing with the usual hexagonal symmetry of the FLL (Ref. 11) and the evidence for thermal melting line of hexagonal FLL to lie in infinitesimal close proximity (within a few millikelvin) of the upper critical field line $[H_{c2}(T)]$ (Ref. 8). Identification of peak-effect phenomenon with direct structural evidence related to an order-disorder transition in the FLL correlations, supercooling and superheating effects[7] across this transition, survival of surface superconductivity[10,12] well above this transition, etc. have been intriguing observations in another Nb crystal with weak pinning. Historically, reports on peak-effect phenomenon and surface superconductivity in high-purity thin wires of Nb have existed in literature for a long time.[13–19] In addition, there have been numerous reports of positive magnetization signal on field cooling superconducting specimen of different variety.[20–23] In the context of high T_c cuprate superconductors[20,21,24] (HTSC), the Meissner-type diamagnetic response on the application of a magnetic field is typically found only in the zero-field cooled (ZFC) state; on field cooling (FC), a HTSC sample often shows paramagnetic magnetization at low fields. Such an observation is designated as paramagnetic or inverse Meissner effect and sometimes as Wohlleben effect.[20,21] The origin of this paramagnetic Meissner effect in cuprate superconductors has been considered to intimately relate to their unconventional superconductivity.[25–27] Some theories indicate that the existence of spontaneous Josephson currents, generated at π junctions across some grain boundaries in the sample, lead to the observation of the positive magnetization in a superconductor. While such a scenario may hold for HTSC, the later observations of positive magnetization signal even in the conventional low T_c superconductors, such as single crystals of Nb (Refs. 22 and 23) and nanostructured Al disks,[28] imply that the effects other than the π junctions and the unconventional superconductivity can also be the source of positive magnetization signal on field cooling. Some ideas[29,30] suggest that such a paramagnetic signal can be related to magnetic flux trapping and its compression inside a superconductor. The flux trapping leading to positive signal could result from inhomogeneities on the surface of the superconductor, geometry effects or inhomogeneous cooling of the sample. Very many issues related to the possible underlying connection between positive field cooled magnetization regime, surface superconductivity, FLL melting, peak-effect (PE) phenomenon that quintessentially marks the order-disorder transition for pinned vortices, the role of intrinsic superconducting parameters in delineating observed different features, etc. have not received a desired amount of attention.[10] We propose to focus here on a part of these emergent issues via explorations in a specially grown spherical single crystal sample of Nb.

II. EXPERIMENTAL

A source of disorder, while growing a single crystal, can be an unavoidable reaction between the sample melt and the container hearth. To overcome this, as well as to minimize irregularities on the surface, Nb single crystals were grown under containerless condition.[31] Such a condition was achieved by levitating an electrostatically charged flux and initiating the melting with laser irradiation in high vacuum. The details are described in Ref. 31. We have recorded the ac and dc magnetization data on one of the above stated high-quality single crystals of Nb ($T_c \sim 9.3$ K, mass=49.1 mg) with a spherical shape (radius 1.4 mm). The crystal was mounted so as to conveniently apply a dc field along the crystallographic [100] direction of the cubic structure of Nb. The dc magnetization and ac susceptibility data were re-

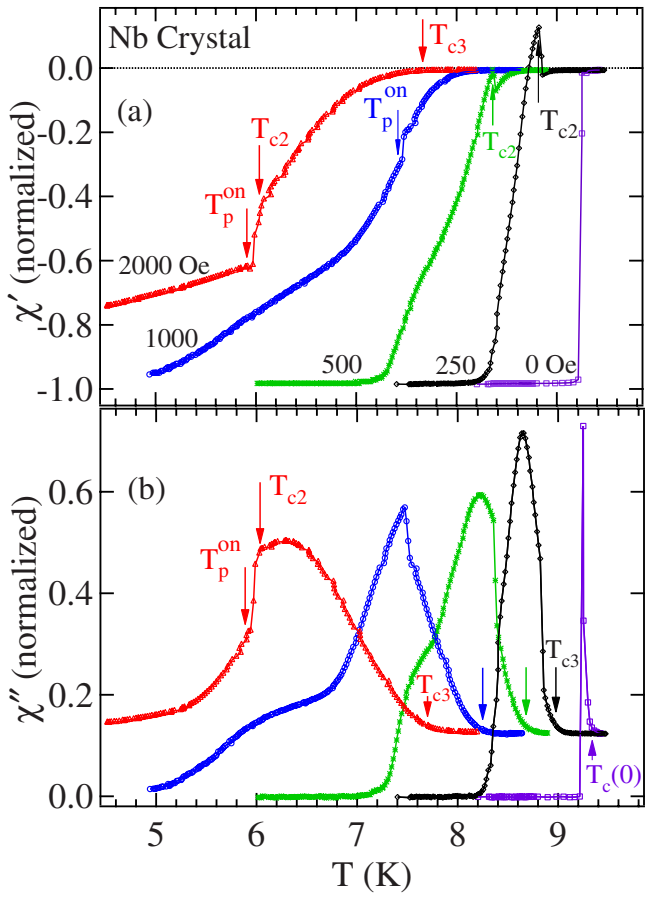

FIG. 1. (Color online) Panels (a) and (b), respectively, show the temperature variation of the in-phase (χ') and the out-of-phase (χ'') ac [f=211 Hz and h_{ac}=2.5 Oe (rms)] susceptibility in a spherical single crystal of Nb for $H\|[100]$ at the fields, as indicated. The zero-field transition temperature $T_c(0)$ is indicated in the χ'' data for H=0. The representative values of T_p^{on}, T_{c2}, and T_{c3} have been marked for H=2000 Oe (see text).

corded using vibrating sample magnetometer (VSM) and ac susceptibility options, respectively, in a Physical Properties Measurement System (PPMS, Quantum Design Inc., USA).

III. RESULTS

Figures 1 and 2 show representative plots of temperature variation of ac susceptibility (f=211 Hz, h_{ac}=2.5 Oe) and dc magnetization (M), respectively, in the Nb crystal for $H\|[100]$. The in-phase ac susceptibility (χ') plots are normalized, such that in nominal zero field, $\chi'=-1$ [cf. Fig. 1(a)] and the out-of-phase ac susceptibility (χ'') data are plotted such that the dissipation response vanishes deep in the superconducting state [cf. Fig. 1(b)]. The inset panel (a) in Fig. 2 shows a typical $M(T)$ plot in the field cool warm up (FCW) mode at 750 Oe. The main panel and the inset panel (b) in Fig. 2 show expanded portions of the FCW $M(T)$ plots at different fields (up to 2625 Oe), close to the respective superconducting transition temperatures, thereby, enabling the identification of the positive field cooled magnetization (PFCM) feature for each curve.

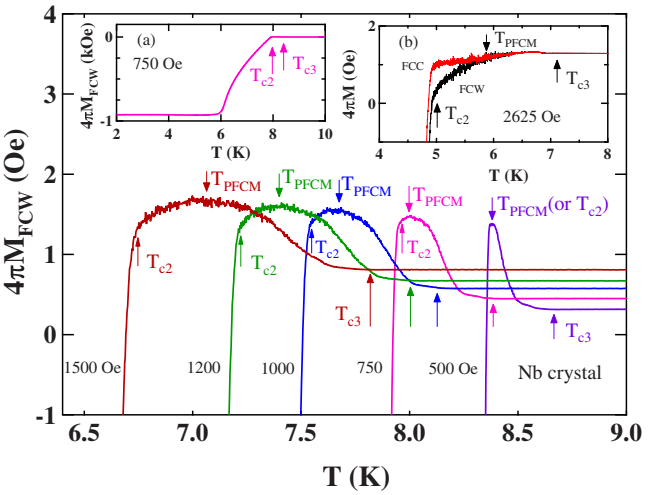

FIG. 2. (Color online) Inset panel (a) shows the temperature variation of FCW magnetization in H=750 Oe in a spherical single crystal of Nb for $H\|[100]$. The main panel and the inset panel (b) show the $M_{FCW}(T)$ curves in different fields on an expanded scale. T_{c3} and T_{c2} values marked were obtained from χ' and χ'' plots in Fig. 1. $T_{PFCM}(T)$ values in $M_{FCW}(T)$ plots notionally identify the onset of diamagnetic response during dc magnetization runs (see text). The inset panel (b) also includes an expanded portion of the FCC magnetization curve, $M_{FCC}(T)$, in H=2625 Oe; such curves in other field values are not being displayed. The difference between $M_{FCW}(T)$ and $M_{FCC}(T)$ curves between T_{c2} and T_{PFCM} progressively decreases as H decreases from 2625 to 1000 Oe. At 750 Oe, $T_{c2}(H)\rightarrow T_{PFCM}(H)$ and the said difference vanishes.

$\chi'(T)$ curve in H=0 Oe [cf. Fig. 1(a)] shows the diamagnetic shielding response rapidly reaching its saturation limit across $T\sim 9.2$ K. At that temperature, the corresponding $\chi''(T)$ curve in Fig. 1(b) displays a sharp maximum, and above it, the χ'' value merges into the background normal state response at 9.3 K, which we mark as $T_c(0)$. In the same spirit, we locate the superconducting transition temperatures at different fields by the merger of $\chi''(T)$ values to the respective background responses in Fig. 1(b). These temperatures have been designated as T_{c3} in Fig. 1(b), in view of the observed characteristic feature in $\chi'(T)$ and $\chi''(T)$ deeper inside the superconducting state. The shape of $\chi'(T)$ response at H=2000 Oe in Fig. 1(a) is reminiscent of a similar behavior observed by Park *et al.*[10] in their crystal of Nb, wherein a tiny anomalous enhancement (at T_p^{on}) in the diamagnetic response (due to PE) is accompanied by a sharp drop, followed by a gradual decrease in the diamagnetic response, to eventually merge into the near zero response in the normal state. The onset of an anomalous increase in $\chi'(T)$ at a temperature marked as T_p^{on} characterizes the quintessential peak-effect phenomenon, which is a precursor to the arrival of the upper critical field line. The PE marks the collapse of elasticity of the flux line lattice, concurrent to the collapse of pinning in the bulk of the crystal, while approaching the upper critical field line. Consistent with Park *et al.*,[10] a temperature value just above the PE region, where there is an apparent change in the curvature of $\chi'(T)$ response, has been indicated as T_{c2}. Above T_{c2}, the diamagnetic response in $\chi'(T)$ is due to the phenomenon of surface

superconductivity,[10] which survives up to the arrival of the normal state at T_{c3}. The fingerprint(s) of crossing T_{c2} during the temperature variation runs can be noted in the $\chi''(T)$ curves of Fig. 1(b) from high field down to $H=1000$ Oe. At fields lower than about 750 Oe, we could not distinctly resolve the PE anomaly in $\chi'(T)$ curves. However, the crossover from surface superconductivity to the creation of vortices in the bulk of the sample can be identified via a sudden enhancement in the dissipative $\chi''(T)$ responses. For example, see the $\chi''(T)$ curves at $H=500$ Oe and 250 Oe in Fig. 1(b) and the marking of T_{c2} values in the corresponding $\chi'(T)$ curves in Fig. 1(a). It is interesting to note that for $H<750$ Oe, $\chi'(T)$ response between T_{c2} and T_{c3} values is a consequence of the fluctuations between diamagnetic and (effective) paramagnetic responses, which implies the emergence of distinct metastability in the response with the crossover from bulk to surface superconductivity at such fields.[28]

We now focus our attention onto the $M(T)$ curve at $H=750$ Oe in the inset panel and a part of it expanded in the main panel of Fig. 2. At the lowest temperature, the applied field (750 Oe) is largely excluded from the sample resulting in a large saturated diamagnetic response. As the applied field of 750 Oe exceeds the effective lower critical field $H_{c1}(T)$ near 6 K, the saturated shielding response starts to decrease [cf. inset panel (a), Fig. 2], while raising temperature toward T_{c2}. The expanded portion of the plot at $H=750$ Oe in the main panel of Fig. 2 clearly shows that the diamagnetic response crosses over to a paramagnetic response, which then decreases again and merges into the background (paramagnetic) normal state value at $T=T_{c3}$. The paramagnetic peak below T_{c3} notionally identifies the PFCM signal. We could witness the PFCM in our spherical Nb crystal up to fields as large as 3600 Oe. Note that the width of the PFCM region enhances as the applied field is increased from 500 Oe. The magnetization values in the normal state ($T>T_{c3}$) scale linearly with H and hence the background paramagnetic signal also enhances with H. This perhaps limits the unambiguous identification of PFCM (as an excess signal over normal state value) at fields higher than 3600 Oe. We have marked by arrows the limiting temperature values, T_{PFCM}, below which the diamagnetism is seen to set in at a chosen field in the dc magnetization response. The field values (for $H\geq 1000$ Oe), where we witness the PE [marked as T_{c2}, obtained from the $\chi'(T)$ plots in Fig. 1], are significantly different from the respective $T_{\mathrm{PFCM}}(H)$ values in Fig. 2. At lower fields ($H<750$ Oe), the $T_{c2}(H)$ values [noted from $\chi''(T)$ plots in Fig. 1] move progressively closer to the respective $T_{\mathrm{PFCM}}(H)$ values. At $H=500$ Oe, the $T_{\mathrm{PFCM}}(H)$ and $T_{c2}(H)$ values are nearly the same.

Figure 3 shows a portion of the five quadrant hysteresis (M-H) loop recorded in the Nb sphere at 2 K, where only the virgin ZFC forward curve in the first quadrant and the reverse leg in the second quadrant have been depicted. The initial portion of the M-H curve can be utilized to determine the threshold of lower critical field using the deviation from linearity criterion. At 2 K, H_{c1} in the given Nb sphere is 1052 Oe. The determination of $H_{c1}(T)$ at different temperatures and their fit to the equation $H_{c1}=H_{c1}(0)[1-(T/T_c)^2]$ yielded the extrapolated $H_{c1}(0)$ value to be ~1100 Oe, which compares favorably with values reported in literature[10] in the

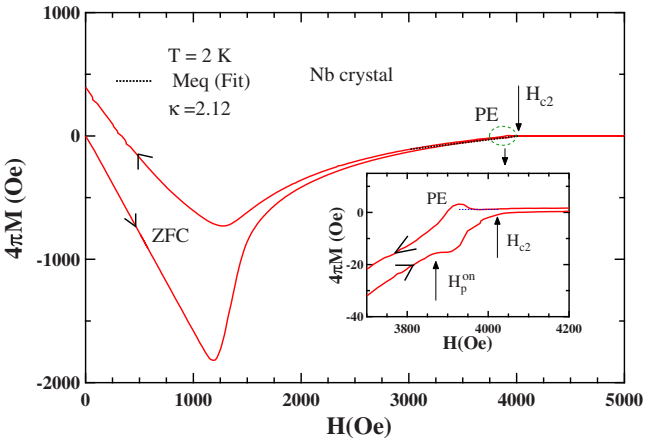

FIG. 3. (Color online) A portion of the dc magnetization hysteresis curve in a spherical single crystal of Nb for $H\|[100]$ at 2 K. The black dashed line in the main panel shows the Ginzburg-Landau fit of the equilibrium magnetization to the experimentally determined equilibrium magnetization (see text). The inset panel shows a portion of the M-H curve across the peak-effect region on an expanded scale. The onset of the PE (H_p^{on}) and the upper critical field (H_{c2}) have been identified.

clean crystals of Nb. It can be noted that the M-H loop is largely reversible above 1500 Oe, which attests to the weak pinning characteristic of the given crystal. However, there is a small finite residual pinning in the bulk of the sample for $H>3000$ Oe. The inset panel in Fig. 3 shows a portion of the M-H loop on an expanded scale between 3700 and 4200 Oe, in which the enhancement of the magnetization hysteresis at ~3900 Oe can be clearly noted as a fingerprint of the PE phenomenon in the dc magnetization data, where it pertains to the currents sustained in the bulk of the sample. The quasi-reversible magnetization values prior to the PE region can be utilized to attempt a fitting to the relationship given by Brandt in Ref. 6, viz., $M_{\mathrm{eq}}=-(H_{c2}-H)/1.16(2\kappa^2-1)$, where κ is the ratio of the penetration depth and the coherence length and H_{c2} is the upper critical field. The dotted black line in Fig. 3 is a fit to the above relation which yields $\kappa=2.12$ using $H_{c2}(2\ \mathrm{K})=4020$ Oe.

Figure 4 presents a collation of all the temperatures (and/or fields) corresponding to the onset position of the PE (H_p^{on}), the superconductivity in the bulk (T_{c2}), the threshold for positive field cooled magnetization (T_{PFCM}) and the onset of surface superconductivity (T_{c3}), along with the determined values of $H_{c1}(T)$, in a field-temperature (H-T) phase diagram. Different regions of the phase space have been identified with different characteristics of the flux line lattice in the given Nb sphere; the nomenclature is self-evident. If the lines drawn in Fig. 4 are assumed as phase boundaries, we do not find any multicritical point, where H_p^{on}, T_{c2}, and T_{c3} lines could meet, as was noted by Park *et al.*[10] in their crystal of Nb, which also showed the PE and surface superconductivity. If instead of the $T_{c2}(H)$ line, we take the $T_{\mathrm{PFCM}}(H)$ line determined using the criterion of the onset of diamagnetic response in the dc magnetization data to be a phase boundary, it would also not meet the $T_p^{\mathrm{on}}(H)$ line, which terminates at the low field end ($H<1000$ Oe).

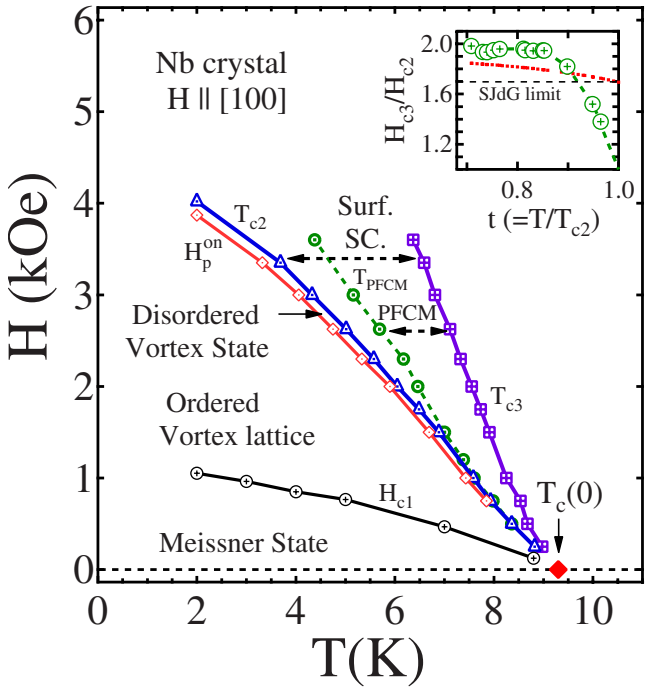

FIG. 4. (Color online) Field-temperature (H,T) vortex phase diagram in a spherical single crystal of Nb for $H\|[100]$. The H_{c1}, order-disorder, T_{c2} and T_{c3} lines have been drawn as solid curves, whereas a dotted curve passes through $T_{\mathrm{PFCM}}(H)$ data. An inset panel shows a plot of H_{c3}/H_{c2} versus $T/T_c(0)$ along with a curve (red online) drawn based on a relationship due to Hu and Koreman (Ref. 32). The data points correspond to the values chosen from the $T_{c3}(H)$ and $T_{c2}(H)$ lines drawn in the main panel of Fig. 4. The horizontal dashed line identifies the SJdG limiting value of 1.695 for H_{c3}/H_{c2}, as predicted by Saint-James and de Gennes (Ref. 12).

IV. DISCUSSION

A. Surface superconductivity and peak effect in niobium: Early work

Saint-James and de Gennes (SJdG) (Ref. 12) had predicted that the superconductivity within a surface layer of thickness about the coherence length (ξ) can exist up to about $1.7H_{c2}$, when magnetic field is applied to a vacuum-superconducting interface of radius of curvature greater than ξ. Finnemore, Stromberg and Swenson (FSS) (Ref. 16) explored the existence of surface superconductivity in high-purity (polycrystalline) samples of elemental niobium in the form of very thin wires and found its presence in several of them via ac susceptibility signals surviving above the notional H_{c2} values. The high-purity samples studied by FSS had $\kappa\sim 1$ and yielded largely reversible dc magnetization hysteresis curves. Hopkins and Finnemore (HF) (Ref. 17) studied the effect of Ta doping from 10^2 ppm to 2×10^4 ppm in high-purity niobium specimen in the form of thin wires and explored the correlation between the H_{c3}/H_{c2} ratio and the electronic mean free path (l) in the light of a prediction by Hu and Koreman (HK) (Ref. 32) that the said ratio at low temperature would be well above 1.7 K in the limit of large l values. In the highest purity Nb specimen having ~ 100 ppm Ta impurity, the ratio H_{c3}/H_{c2} was determined to be above 1.8 at the lowest temperature $[T/T_c(0)\sim 0.6]$, and it decreased very slowly while raising the temperature up to about $T/T_c(0)\sim 0.9$, in reasonable accordance with the theory of HK.[32] HF reported that $T_c(0)$, l, and H_{c2} values show expected variations with progressive increases in the Ta impurity content, viz., $T_c(0)$ marginally lowered, l rapidly decreased (from $\sim 10^5$ to $\sim 10^3$ Å) and H_{c2} values somewhat increased. However, the values of the ratio H_{c3}/H_{c2} were observed to remain distinctly above the SJdG limit of 1.7 up to about $T/T_c(0)\sim 0.85$, for Ta impurity $\sim 5\times 10^3$ ppm (cf. Fig. 5 of Ref. 17).

No fingerprint of PE was evident in the field dependence of the in-phase (χ') and/or the out-of-phase (χ'') ac susceptibility data at different temperatures in the samples of varying purity studied by HK.[32] Autler, Rosenblum and Gooen (ARG) (Ref. 13) had, however, earlier reported surfacing of PE in several thin wire samples of Nb. In their highest purity sample having largest residual resistivity ratio (RRR of ~ 100) and the lowest H_{c2} value (at a given temperature), the PE anomaly is very deep and sharp. The κ value in the said sample is about 1.3. In the data of ARG, one can note that, as the effect of disorder grows (as reflected by the decrease in values of RRR), the upper critical field values increase and the PE anomaly progressively turns less sharp. In specimen having large critical current density ($>10^4$ A/cm^2 at $H\sim 1$ kOe), the PE anomaly is conspicuously absent. However, the fingerprint of surface superconductivity is evident in all the samples studied by ARG above the nominal H_{c2} value.[13] Surface pinning effect surviving above H_{c2} values can be noted in the Nb samples investigated by DeSorbo[14,15] as well. DeSorbo studied the effect of substitutional and interstitial impurities on the PE phenomena in Nb wires via dc magnetization hysteresis and electrical resistivity measurements in longitudinal and transverse (field applied perpendicular to the length of the wire) geometries. He reckoned that the PE was robust when the pinning was optimally weak. The PE anomaly was absent in pinning-free as well as strongly pinned samples having significantly larger H_{c2} values than the purest sample. As regards to the values of H_{c3}/H_{c2}, DeSorbo summarized that the said ratio $(\sim 1.6-1.7)$ was independent of the κ value for pure Nb as well as for low oxygen content (<0.7 at. %) Nb samples.

As far as the properties of single crystal samples of Nb are considered, Freyhardt[18] found that the disorder introduced by twisting of the single crystal enhanced its upper critical field with respect to its pristine state and nucleated the fingerprint of the PE anomaly in the isothermal magnetization hysteresis loop. Kartascheff[33] reported the onset of a sharp PE anomaly in the M-H loops measured for bulk cylindrical Nb sample in which the pinning effects at the surface inhomogeneities had been eliminated. There is no evidence of surface superconductivity above H_{c2} in Ref. 33. We shall compare and contrast the observed behavior in our spherical Nb single crystal with the above descriptions after discussion on peak-effect phenomenon in context of different phases of vortex matter in Sec. IV B.

B. Peak effect and the vortex phase diagram

The advent of high T_c era brought focus on the peak-effect phenomenon as a fingerprint of a first-order-like phase

transition between the ordered and disordered phases of vortex matter in low T_c superconductors such as 2H-$NbSe_2$, $CeRu_2$, etc.[34–36] In this context, Ling *et al.*[7] provided direct structural evidence in support of the supercooling/superheating effects across the phase boundary of the PE line via small angle neutron scattering (SANS) studies in a single crystal of high-purity cylindrical Nb sample for field applied parallel to [111] axis of the crystalline lattice. Subsequently, Park *et al.*[10] found the presence of surface superconductivity in the same crystal and they sketched its vortex phase diagram, where they also articulated the notion of a multicritical point stated earlier in Sec. III. The H_{c3}/H_{c2} ratio at low temperatures is reckoned to be about 1.6 in their crystal by Park *et al.*[10] Meanwhile, Forgan *et al.*[8] reported SANS studies in another very high-purity Nb crystal ($\kappa \sim 1.57$ at 5.2 K), where RRR value was $\sim 10\,000$ corresponding to l/ξ of about 1000 and which had H_{c2} values much lower (about half) than those in the crystal of Ling *et al.*[7] Forgan *et al.*[8] did not observe any structural phase transition *a la* PE phenomenon up to T_{c2} for their hexagonal flux line lattice obtained in $H=2$ kOe. In another recent study on a Nb single crystal ($T_c \approx 9.2$ K, $\kappa \sim 1.5$), Tsindlekht *et al.*[37] observed surface superconductivity with an H_{c3}/H_{c2} ratio of 2.34 at 4.5 K [$t=T/T_{c2}(0)=0.48$], reducing to about 1.9 at 8.5 K ($t=0.92$). There are no data on the PE phenomenon and/or PFCM signal in Ref. 37.

When we view the experimental results in Figs. 1–4 in the light of discussions summarized above, we reckon that our spherical single crystal sample is optimally weakly pinned, in which the quintessential peak effect is sharp and located at the edge of the upper critical field.[13,37] The low $\kappa(\sim 2)$ as well as low H_{c2} values also place this specimen among the very pure class of niobium samples. To substantiate this notion further, we draw attention to the plot of H_{c3}/H_{c2} vs $t=T/T_{c2}(0)$ for our Nb single crystal in the inset panel of Fig. 4. The data points correspond to the values determined from $T_{c3}(H)$ and $T_{c2}(H)$ lines sketched in the vortex phase diagram in the main panel of Fig. 4. The horizontal dashed line marks the SJdG limit of 1.695, whereas the [red (online)] dotted curve corresponds to a theoretical relationship given by Hu and Koreman[32] having validity at high-temperature end, i.e., as $t \to 1$. As per HK theory, the ratio reaches the SJdG limit at $t=1$, whereas the experimental data in our single crystal as well as in the highest purity Nb wires studied by HF (Ref. 17) show a steep decline above $t \sim 0.9$ (cf. data points in the inset of Fig. 4 in this paper and the curves in Fig. 5 of Ref. 17). HF had attributed the difference between the experimental data and the theoretical curve (due to HK) to the suppression (i.e., the spatial variation) of the superconducting interaction parameter near the sample surface, following a prescription by Hu.[38]

Another check on the purity of our spherical crystal can be through the estimation of the electronic mean free path in it, and its comparison with the coherence length. Using $H_{c2}(0) \sim 4200$ Oe, we estimate the penetration depth $\lambda=417$ Å in our sample, using the expression[16] $\lambda=[\phi_0 H_{c2}/4\pi H_c^2(0)]^{1/2}$, where we have substituted $H_c(0)=1993$ Oe as the thermodynamic critical field of Nb.[4,16] Using[16] the value of London's penetration depth $\lambda_L=350$ Å and BCS $\xi_0=430$ Å in the relationship[39] $\lambda(0)=\lambda_L(0)(1+\frac{\xi_0}{l})^{1/2}$, we obtain the electronic mean free path $l \sim 1000$ Å. Using $\kappa \sim 2$ (deduced earlier) and $\lambda=417$ Å, we estimate the superconducting coherence length $\xi \sim 200$ Å for our sample. The large value of l ($\gg \xi$) indicates that purity-wise, our spherical Nb crystal is at least in the same class as the samples which have been studied in recent years.[7,10]

C. Field cooled positive magnetization response

In the last two decades there have been numerous reports of PFCM response in high T_c cuprates,[20,21,24] particularly in the granular form, where such an effect is attributed to the generation of spontaneous paramagnetic moments.[20,21,26,40] The appearance of spontaneous moments in cuprates is possible due to the unconventional nature of superconductivity in them. In such materials, it is possible that due to crystallographic mismatch across a granular interface, the anisotropic *d*-wave superconducting order parameter develops a mismatch with a particular phase difference across the interface.[25] Due to this particular phase difference, a Josephson current tunnels perpendicular to the grain interface. Such interfaces are called π junctions. The spontaneous Josephson current tunneling perpendicular to the π junctions is responsible for the generation of a spontaneous moment. Analogous to *XY* spin glasses,[41] a random distribution of π junctions in granular materials leads to a frustration[42,43] within the superconducting condensate in the grains. The condensate is referred to as *chiral glass*[43] which exhibits a peculiar low field glassy response. The chiral glass is characterized by spontaneously quenched half-flux quanta at the sites of a local loop of current tunneling across the grains. Observation of memory effects and aging phenomenon[44,45] along with the PFCM in the granular materials is associated with the chiral glass phase. It therefore seems that paramagnetic Meissner effect and/or PFCM signal is very intimately related to the peculiarities of the unconventional superconducting order parameter in cuprate superconductors, and one may not observe any of the above features in samples of conventional superconductors having usual *s*-wave symmetry. The above reasoning was, therefore, discounted while describing the observation of PFCM in clean samples of conventional superconductors such as pure Nb.[22,23]

There is a fair consensus that the PFCM signal in Nb could be due to magnetic flux compression inside the sample. Compression of flux inside the sample could be due to inhomogeneities on the surface of the superconductor or due to inhomogeneous cooling. Koshelev and Larkin[29] considered the effect of inhomogeneous cooling of the superconducting surface as compared to its interior, which can result in shielding currents circulating near the surface of the superconductor, as the reason for flux compression in the interior of the superconductor. The compressed flux generates a paramagnetic moment in the field cooled state. While inhomogeneous cooling is a plausible mechanism, there is another mechanism,[12] viz., that of surface superconductivity, which can produce flux compression and hence paramagnetic field cooled magnetization signal. As shown above, our spherical single crystal of Nb is closer to the purest Nb

samples in several aspects, on which results have been reported in the literature. In exceptionally pure superconductors, superconductivity is expected to nucleate in a thin region of the order of ξ near the surface[12] at a temperature $T \sim T_{c3}(H)$ [equivalent to $H_{c3}(T)$]. The presence of a thin superconducting surface (of thickness$=\xi$) at the boundary of the material as the superconductor is cooled in a field from above $T_{c3}(H)$ would lead to compression of flux within the normal interior in the bulk of the superconductor. This compressed flux may lead to a slight enhancement in the paramagnetic response, well before the diamagnetic signal becomes stronger as the superconductivity permeates in the interior of the sample at $T_{c2}(H)$. Such an argument permits the observation of PFCM along with the fingerprint of surface superconductivity in the overlapping (H,T) phase space.

In nanosized superconductors, one can safely eliminate the possibility of inhomogeneous cooling as the source of observation of PFCM. In fact in nanodisks of Al,[28] the positive field cooled magnetization signal has been observed along with surface superconductivity. However, the issue of inhomogeneous cooling is more difficult to eliminate in the case of bulk samples. In fact, in bulk superconducting Nb, signatures of PFCM and surface superconductivity do not seem to have been documented simultaneously. In this respect, our observation of simultaneous PFCM and surface superconductivity in a single crystal sample is significant as we can now favor the source of flux compression to be predominantly due to surface superconductivity effect rather than due to inhomogeneous cooling of the sample. It was shown[12] that for spherical samples (similar to ours), a superconducting (diamagnetic) surface layer exists, restricted to a band around the equatorial plane. Except this area, the magnetic flux is contained within the bulk of the superconductor at $T > T_{c2}$ [$T_{c2}(H)$ being equivalent to $H_{c2}(T)$] during field cooling (FC). When the sample gets cooled down from T_{c3} to T_{c2}, the width of the diamagnetic sheet on the sample boundary increases and the magnetic flux within the bulk of the sample gets compressed, leading to a paramagnetic response (PFCM).[28–30]

We observe from our data in Fig. 2 that the magnitude of the PFCM progressively weakens as the temperature is decreased or magnetic field is increased. We suggest that the given T (or H) dependence may be related to the proximity between $T_{c3}(H)$ and the actual $T_c(0)$. Let r denote the radius of the superconducting sheet within which the magnetic flux is compressed. During field cooling in low fields, the location of $T_{c3}(H)$ is close to $T_c(0)$ [e.g., $T_{c3}(500\ \text{Oe}) = 8.67$ K, $T_c(0) = 9.3$ K] and hence the width of superconducting surface sheet ($\sim\xi$) can be large (due to the well-known T dependence[39] of ξ). Consequently at low H, r is smaller, implying a greater flux compression, which explains the strong PFCM amplitude at low H or high T. At high H, as $T_{c3}(H) \ll T_c(0)$ [e.g., $T_{c3}(3000\ \text{Oe}) = 6.8$ K], the corresponding width of superconducting surface sheet ($\sim\xi$) is comparatively lower, resulting in a larger r, and hence, a weaker flux compression or in other words a weaker PFCM amplitude. Thus, we suggest that the amplitude of the PFCM signal may depend inversely on r, within which the flux is compressed, and r may have a T dependence of the type $(1-\frac{T_{c3}(H)}{T_c(0)})^{\alpha}$ (where α is a positive power). Above a certain value of H, r does not change drastically and it approaches the radius of the sample and hence the amplitude of the PFCM signal is weak at high fields (or at low T).

It may be pertinent to state here that one can note the presence of paramagnetic signals below $T_c(0)$ in the data of Stamopolos, Speliotis and Niarchae[19] along with the observations of peak effect (and/or the second magnetization peak anomaly) and surface superconductivity in one of their thin-film samples of niobium. The PFCM signal in this highly disordered thin film, which had an unusually large $H_{c2}(0)$ value (>30 kOe) and very high κ value, enhanced as the field was increased (cf. Fig. 6 of Ref. 19), exactly opposite to the trend evident in our weak pinning spherical single crystal sample in Fig. 2, for which we have advanced a plausible explanation above. While surface superconductivity phenomenon seems to be the predominant source of PFCM, our data also imbibe another facet not discussed so far, viz., the observation of distinct path-dependent magnetization response in the vicinity of the onset of PFCM from the low-temperature side in our Nb single crystal; see, e.g., the difference between the field cooled cool down (FCC) and the field cooled warm up (FCW) responses in $H = 2625$ Oe in the inset (b) of Fig. 2. Thus, PFCM not only appears along with surface superconductivity phenomenon but it is also associated with a path-dependent phenomenon, which can display glasslike[37] behavior similar to those found in granular high T_c cuprate materials. While the origin of glassy response in granular materials is perhaps due to the chiral glass phase, we speculate a different origin of the path-dependent response near PFCM in our Nb crystal. It is well accepted that the pinning is a major cause of path-dependent magnetization response in superconducting samples.[46,47] We believe that at $T > T_{\text{PFCM}}(H)$, the flux is in the compressed state due to surface superconductivity. However at $T < T_{\text{PFCM}}(H)$ and in the vicinity of T_{c2}, the compressed magnetic flux can start to redistribute or decompose into quantized flux lines, i.e., vortices. These vortices experience pinning, which could be different in FCC and FCW modes, thereby generating a path dependence observed at fields below the peak of PFCM. Thus, rather than using the rapid of permeation diamagnetism into the bulk of the sample to mark T_{c2}, it may be argued that the onset of the path-dependent magnetization response just below a given $T_{\text{PFCM}}(H)$ corresponds to the nucleation of quantized flux lines in the superconductor. The delineation of possible relationship between path-dependent magnetization between $T_{c2}(H)$ and $T_{\text{PFCM}}(H)$ and the characteristics of surface superconductivity require more detailed studies.

V. CONCLUSION

In conclusion, we have reported the coexistence of surface superconductivity and positive field cooled magnetization in a high-purity spherical single crystal of Nb. The positive field cooled magnetization appears when superconductivity in the bulk ceases; it is observed up to very large fields, however, its relative strength decreases. The appearance of path-dependent magnetization response between $T_{c2}(H)$ and $T_{\text{PFCM}}(H)$, we believe, is an evidence for

the nucleation of vortices in the superconductor before superconductivity permeates in the sample throughout. The residual weak pinning in the bulk of the sample germinates the peak-effect phenomenon at the edge of the upper critical field. The peak effect is not seen at fields less than 750 Oe, whereas, PFCM and surface superconductivity continue to remain prominent down to much lower fields. We have attempted to seek a relationship between the observed field dependence of PFCM signal and the possible temperature dependence of the size of the surface conductivity sheet that *inter alia* also governs the PFCM. A field-temperature phase diagram has been drawn, which comprises the loci of the onset of the peak effect (T_p^{on}), the upper critical field [$T_{c2}(H)$], the PFCM [$T_{\mathrm{PFCM}}(H)$], and the superconducting transition temperature [$T_{c3}(H)$]. There is no evidence of any multicritical point in this diagram.

ACKNOWLEDGMENTS

S.S.B. would like to acknowledge funding from CSIR, DST, and IIT Kanpur.

*tomy@phy.iitb.ac.in
†grover@tifr.res.in
‡satyajit@iitk.ac.in

[1] D. Cribier, B. Jacrot, L. M. Rao, and B. Farnoux, Phys. Lett. **9**, 106 (1964).
[2] J. Schelten, G. Lippmann, and H. Ullmaier, J. Low Temp. Phys. **14**, 213 (1974).
[3] D. K. Christen, H. R. Kerchner, S. T. Sekula, and P. Thorel, Phys. Rev. B **21**, 102 (1980).
[4] P. L. Gammel, U. Yaron, A. P. Ramirez, D. J. Bishop, A. M. Chang, R. Ruel, L. N. Pfeiffer, E. Bucher, G. DAnna, D. A. Huse, K. Mortensen, M. R. Eskildsen, and P. H. Kes, Phys. Rev. Lett. **80**, 833 (1998).
[5] G. Blatter, M. V. Feigel'man, V. B. Geshkenbein, A. I. Larkin, and V. M. Vinkur, Rev. Mod. Phys. **66**, 1125 (1994).
[6] E. H. Brandt, Rep. Prog. Phys. **58**, 1465 (1995).
[7] X. S. Ling, S. R. Park, B. A. McClain, S. M. Choi, D. C. Dender, and J. W. Lynn, Phys. Rev. Lett. **86**, 712 (2001).
[8] E. M. Forgan, S. J. Levett, P. G. Kealey, R. Cubitt, C. D. Dewhurst, and D. Fort, Phys. Rev. Lett. **88**, 167003 (2002).
[9] G. P. Mikitik and E. H. Brandt, Phys. Rev. Lett. **89**, 259701 (2002).
[10] S. R. Park, S. M. Choi, D. C. Dender, J. W. Lynn, and X. S. Ling, Phys. Rev. Lett. **91**, 167003 (2003).
[11] M. Laver, E. M. Forgan, S. P. Brown, D. Charalambous, D. Fort, C. Bowell, S. Ramos, R. J. Lycett, D. K. Christen, J. Kohlbrecher, C. D. Dewhurst, and R. Cubitt, Phys. Rev. Lett. **96**, 167002 (2006).
[12] D. Saint-James and P. de Gennes, Phys. Lett. **7**, 306 (1963).
[13] S. H. Autler, E. S. Rosenblum, and K. H. Gooen, Phys. Rev. Lett. **9**, 489 (1962).
[14] W. DeSorbo, Rev. Mod. Phys. **36**, 90 (1964).
[15] W. DeSorbo, Phys. Rev. **134**, A1119 (1964).
[16] D. K. Finnemore, T. F. Stromberg, and C. A. Swenson, Phys. Rev. **149**, 231 (1966).
[17] J. R. Hopkins and D. K. Finnemore, Phys. Rev. B **9**, 108 (1974), and references therein.
[18] H. C. Freyhardt, Philos. Mag. **23**, 345 (1971).
[19] D. Stamopoulos, A. Speliotis, and D. Niarchos, Supercond. Sci. Technol. **17**, 1261 (2004), and references therein.
[20] W. Braunisch, N. Knauf, V. Kataev, S. Neuhausen, A. Grütz, A. Kock, B. Roden, D. Khomskii, and D. Wohlleben, Phys. Rev. Lett. **68**, 1908 (1992).
[21] S. Riedling, G. Bräuchle, R. Lucht, K. Röhberg, H. v. Löhneysen, H. Claus, A. Erb, and G. Muller-Vogt, Phys. Rev. B **49**, 13283 (1994).
[22] D. J. Thompson, M. S. M. Minhaj, L. E. Wenger, and J. T. Chen, Phys. Rev. Lett. **75**, 529 (1995).
[23] P. Kostić, B. Veal, A. P. Paulikas, U. Welp, V. R. Todt, C. Gu, U. Geiser, J. M. Williams, K. D. Carlson, and R. A. Klemm, Phys. Rev. B **53**, 791 (1996).
[24] P. Svedlindh, K. Niskanen, P. Norling, P. Nordblad, L. Lundgren, B. Lönnberg, and T. Lundström, Physica C **162-164**, 1365 (1989).
[25] M. Sigrist and T. M. Rice, Rev. Mod. Phys. **67**, 503 (1995).
[26] D. Dominguez, E. A. Jagla, and C. A. Balseiro, Phys. Rev. Lett. **72**, 2773 (1994).
[27] F. V. Kusmartsev, Phys. Rev. Lett. **69**, 2268 (1992).
[28] A. K. Geim, S. V. Dubonos, J. G. S. Lok, M. Henini, and J. C. Maam, Nature (London) **396**, 144 (1998).
[29] A. E. Koshelev and A. I. Larkin, Phys. Rev. B **52**, 13559 (1995).
[30] V. V. Moshchalkov, X. G. Qiu, and V. Bruyndoncx, Phys. Rev. B **55**, 11793 (1997).
[31] Y. S. Sung, H. Takeya, K. Hirata, and K. Togano, Appl. Phys. Lett. **82**, 3638 (2003).
[32] C. R. Hu and V. Korenman, Phys. Rev. **185**, 672 (1969).
[33] N. Kartascheff, J. Low Temp. Phys. **21**, 203 (1975).
[34] M. J. Higgins and S. Bhattacharya, Physica C **257**, 232 (1996), and references therein.
[35] S. Mohan, J. Sinha, S. S. Banerjee, and Y. Myasoedov, Phys. Rev. Lett. **98**, 027003 (2007).
[36] S. S. Banerjee, A. K. Grover, M. J. Higgins, G. I. Menon, P. K. Mishra, D. Pal, S. Ramakrishnan, T. V. C. Rao, G. Ravikumar, V. C. Sahni, S. Sarkar, and C. V. Tomy, Physica C **355**, 39 (2001), and references therein.
[37] M. I. Tsindlekht, G. I. Leviev, V. M. Genkin, I. Felner, Y. B. Paderno, and V. B. Filippov, Phys. Rev. B **73**, 104507 (2006).
[38] C. R. Hu, Phys. Rev. **187**, 574 (1969).
[39] M. Tinkham, *Introduction to Superconductivity*, 2nd ed. (McGraw-Hill, New York, 1996).
[40] M. A. López de la Torre, V. Peña, Z. Sefrioui, D. Arias, C. Leon, J. Santamaria, and J. L. Martinez, Phys. Rev. B **73**, 052503 (2006).
[41] H. Kawamura, Phys. Rev. B **51**, 12398 (1995).
[42] H. Kawamura, J. Phys. Soc. Jpn. **64**, 711 (1995).
[43] H. Kawamura and M. S. Li, Phys. Rev. Lett. **78**, 1556 (1997).
[44] E. L. Papadopoulou, P. Nordblad, P. Svedlindh, R. Schöneberger, and R. Gross, Phys. Rev. Lett. **82**, 173 (1999).
[45] M. S. Li, P. Nordblad, and H. Kawamura, Phys. Rev. Lett. **86**, 1339 (2001).
[46] G. Ravi Kumar and P. Chaddah, Pramana **31**, L141 (1988).
[47] J. R. Clem and Z. Hao, Phys. Rev. B **48**, 13774 (1993).